Clinical Chemistry 50:10
1748–1754 (2004)

Sensitivity and Specificity of Single-Nucleotide Polymorphism Scanning by High-Resolution Melting Analysis

Gudrun H. Reed and Carl T. Wittwer*

Background: **Screening for heterozygous sequence changes in PCR products, also known as "mutation scanning", is an important tool for genetic research and clinical applications. Conventional methods require a separation step.**

Methods: **We evaluated the sensitivity and specificity of homogeneous scanning, using a saturating DNA dye and high-resolution melting. Heterozygous single-nucleotide polymorphism (SNP) detection was studied in three different sequence backgrounds of 40%, 50%, and 60% GC content. PCR products of 50–1000 bp were generated in the presence of LCGreen™ I. After fluorescence normalization and temperature overlay, melting curve shape was used to judge the presence or absence of heterozygotes among 1632 cases.**

Results: **For PCR products of 300 bp or less, all 280 heterozygous and 296 wild-type cases were correctly called without error. In 672 cases between 400 and 1000 bp with the mutation centered, the sensitivity and specificity were 96.1% and 99.4%, respectively. When the sequence background and product size with the greatest error rate were used, the sensitivity of off-center SNPs (384 cases) was 95.6% with a specificity of 99.4%. Most false negatives occurred with SNPs that were compared with an A or T wild type sequence.**

Conclusions: **High-resolution melting analysis with the dye LCGreen I identifies heterozygous single-base changes in PCR products with a sensitivity and specificity comparable or superior to nonhomogeneous techniques. The error rate of scanning depends on the PCR product size and the type of base change, but not on the position of the SNP. The technique requires only PCR reagents, the dye LCGreen I, and 1–2 min of closed-tube, post-PCR analysis.**

Many genotyping methods are available, including closed-tube methods that use probes to generate allele-specific melting curves *(1–3)*. These melting methods can be used to detect any sequence alteration under the probe and are more powerful than methods that detect only a single allele *(4)*. However, sequence variants outside of the probe region are not detected. A closed-tube, homogeneous melting method that would detect any sequence variant within a PCR product would provide a simple screening method for sequence alterations.

Conventional mutation scanning methods require a separation step and include single-strand conformational polymorphism (SSCP) analysis *(5)*, denaturing gradient gel electrophoresis *(6)*, heteroduplex analysis *(7)*, denaturing HPLC *(8)*, and temperature gradient capillary electrophoresis *(9)*. These methods require separation of PCR products on a gel or other matrix, often take hours to perform, and increase the risk of contamination in future reactions because PCR products are exposed to the environment.

Certain dyes that stain double-stranded DNA are compatible with PCR at high concentrations and allow closed-tube detection of heteroduplexes *(10)*. After PCR amplification of heterozygotes, four duplexes are formed: two homoduplexes and two heteroduplexes. Each duplex has a characteristic melting temperature, and the sum of all transitions can be observed by melting curve analysis. The presence of heteroduplexes changes the melting curve shape of amplified heterozygotes compared with homozygotes. The changes are small but can be reliably detected with high-resolution melting analysis. The technique has been applied to single-nucleotide polymorphism (SNP) typing *(11)*, unlabeled probe genotyping *(3)*, HLA matching *(12)*, and mutation scanning for the *MCAD (13)* and c-*kit (14)* genes.

To estimate the sensitivity and specificity of high-

Department of Pathology, University of Utah Medical Center, 5B418, 50 N. Medical Dr., Salt Lake City, UT 84132.

*Author for correspondence. Fax 801-581-4517; e-mail carl.wittwer@path.utah.edu

Received June 17, 2004; accepted July 14, 2004.

Previously published online at DOI: 10.1373/clinchem.2003.029751

resolution melting analysis for mutation scanning of heterozygous single-base changes, we used a previously developed DNA "Toolbox" *(7)*. The Toolbox allows systematic study of the effects of PCR product size, specific base change, GC content, and position of the base change within the PCR product.

Materials and Methods

DNA TOOLBOX

Plasmids from the DNA Toolbox were kindly provided by Cambrex BioScience (Rockland, ME). The design and use of the Toolbox have been published *(7)*. Briefly, 800- to 1000-bp regions in common cloning vectors with approximate GC contents of 40%, 50%, and 60% were identified in M13, λ, and pBR322, respectively. For each vector, four possible nucleotides (A, C, G, or T) were placed at one position by site-directed mutagenesis, giving 12 different constructs. Each construct was then inserted into a pUC19 or pCR2.1 plasmid, and the sequence was verified. Theoretical stability simulations *(6)* of these regions centered at the variable site of each insert are shown in Fig. 1. The concentration of each plasmid was determined by absorbance at 260 nm (A_{260}), assuming an A_{260} of 1.0 is 50 mg/L.

PRIMERS

For products of ~100, 200, 300, 400, 500, and 600 bp with the variable site positioned near the middle, the previously reported primers were used *(7)*. Additional primers were also designed to amplify ~50-bp products for M13 (5′-GCATTTGAGGGGGATTCAATGA-3′ and 5′-CAATACTGCGGAATCGTCATAAATA-3′), λ (5′-CTCTGCGGCTTTCTGTT-3′ and 5′-AGTAAAAGCTCTTGGATTCCTG-3′), and pBR322 (5′-CGGAATCTTGCACGCCCT-3′ and 5′-GGTGGCGGGACCAGTG-3′); ~700-bp products for M13 (5′-GTTACATGGAATGAAACTTCCAG-3′ and 5′-ATTGTGAATTACCTTATGCGA-3′); ~800-bp products for M13 (5′-TCAAACTAAATCTACTCGTTCGC-3′ and 5′-TGCCCTGACGAGAAACA-3′), λ (5′-CACTGCATAAACCATCGG-3′ and 5′-CGTTACCGAATGGATGG-3′), and pBR322 (5′-GTTTCGGCGTGGGTATGGT-3′ and 5′-ATCCATGCCAACCCGTTCC-3′); and ~1000-bp products for M13 (5′-AATTGATGCCACCTTTTCA-3′ and 5′-CCTTCATCAAGAGTAATCTTGAC-3′), all with the SNP approximately centered. The position of the sequence variation was studied by selecting two PCR primers at different distances from the SNP site. Oligonucleotide primers were synthesized by standard phosphoramidite chemistry by our local core facility (University of Utah).

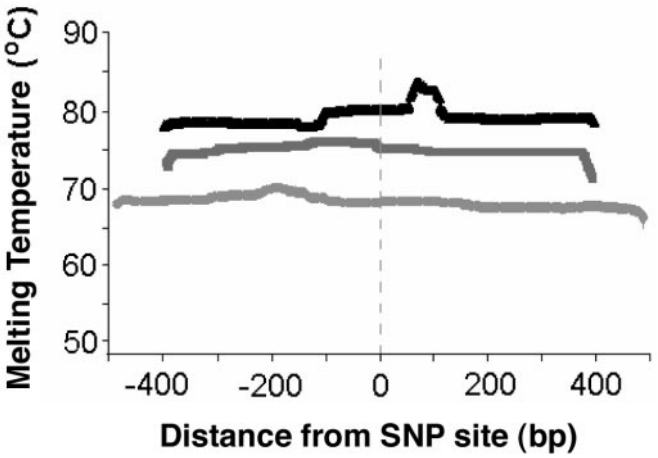

Fig. 1. Computational melting simulation of the three targets analyzed *(6)*.

The M13 sequence (~40% GC) is in *light gray*, the λ sequence (~50% GC) is in *dark gray*, and the pBR322 sequence (~60% GC) is in *black*. Because the simulation assumes different conditions (e.g., salt and DNA concentrations) than those used experimentally, the absolute temperatures predicted by the simulation are lower than those actually observed (see Figs. 2, 3, and 6).

PCR PROTOCOL

PCR was performed in 10-μL volumes in a LightCycler (Roche Applied Science) with programmed transitions of 20 °C/s unless otherwise indicated. The amplification mixture included 2 mM Mg^{2+}, 50 mM Tris-HCl (pH 8.3), 500 mg/L bovine serum albumin, 200 μM each deoxynucleotide triphosphate, 0.5 μM each of two primers, plasmid DNA at 10^5 copies per reaction, 0.4 U of KlenTaq1 Polymerase (AB Peptides), 88 ng of TaqStart antibody (ClonTech), and 1× LCGreen™ I (Idaho Technology). PCR cycling conditions varied with the target.

The temperature cycling protocol included an initial denaturation step at 95 °C for 8 s, followed by 35 cycles of denaturation at 95 °C for 0 s, annealing for 0 s, and extension at 72 °C with a transition from annealing to extension of 2 °C/s. For the M13 (40% GC), λ (50% GC), and pBR322 (60% GC) constructs, the annealing temperatures were 50, 55, and 60 °C, respectively. The extension times were 0, 5, 10, 15, and 30 s for the products of 50, 100–200, 300–400, 500–600, and 700-1000 bp, respectively.

Although not necessary for mutation scanning, the reactions were monitored during PCR at the end of each extension phase in the F1 channel of the LightCycler. As a check on template concentration, the crossing points of the four homozygous PCR products of each primer pair were required to be within a factor of 2. The second-derivative maximum method was used for crossing point determination *(15)*.

HETERODUPLEX FORMATION AND MELTING CURVE ANALYSIS

After amplification, the samples were heated momentarily in the LightCycler to 94 °C and cooled to 50 °C at a programmed rate of 20 °C/s. The LightCycler capillaries were then transferred to a high-resolution melting instrument (HR-1; Idaho Technology), and melting curves were obtained by heating from 70 to 95 °C at 0.3 °C/s. High-resolution melting data were analyzed with HR-1 software by fluorescence normalization and temperature overlay as described previously *(16)*.

STUDY DESIGN

Homozygous genotypes (AA, CC, GG, and TT) were obtained by use of one of the Toolbox constructs as template. By mixing equal amounts of two different constructs, we simulated six heterozygous genotypes (AC, AG, AT, CG, CT, and GT). To assess sensitivity and specificity, we performed 22 amplifications with each of the primer pairs, 4 of each homozygote and 1 of each heterozygote. One investigator with knowledge of the genotype then arranged these samples into 24 different sets of four samples, each containing two "wild-type" homozygotes and two unknowns. Six of the sets used AA as wild type, six CC, six GG, and six TT, allowing all possible pairs of the four homozygous amplifications to be used as wild-type calibrators (for study design details, see the Data Supplement that accompanies the online version of this article at http://www.clinchem.org/content/vol50/issue10/). The unknown samples were either wild-type or heterozygous SNPs with one "allele" shared with the wild type. Within the six sets sharing the same wild type, the 12 unknowns were randomly assigned by one investigator to include from 3–9 wild-type samples, the remainder being heterozygotes. Within any set, zero, one, or two of the unknowns were wild type, although within the six sets sharing the same wild type, each of the three heterozygotes was present at least once and the ratio of wild-type to mutant unknowns varied between 25% and 75%, with a mean of 50%. For each set, the two wild-type samples were identified for the blinded investigator. Using this information, the blinded investigator was required to identify the unknowns as either wild type or mutant.

The effect of PCR product size was studied from 50 to 1000 bp with the mutation near the center, including 576 cases with products of 300 bp or less and 672 cases with products between 400 and 1000 bp. The effect of SNP position was studied in 384 additional cases, using the PCR product with the highest error rate when the sequence alteration was centered.

Results

High-resolution melting analysis reveals differences in melting curve shape that correlate to genotype and the presence of SNP heterozygotes. Shown in Fig. 2 are melting curves from homozygous and heterozygous 100-bp products overlaid at high temperature to visually aid comparison. Homozygous samples have the sharpest melting transitions, whereas melting curves of SNP heterozygotes show broader transitions because the duplexes formed are heterogeneous, including lower-melting heteroduplexes. Furthermore, different heterozygotes produce different curve shapes because different heteroduplexes are formed.

Similar melting curves from a typical 600-bp product are shown in Fig. 3. This larger product melts in two stages. The sequence variation is in the domain with the higher melting temperature, and the curves are best

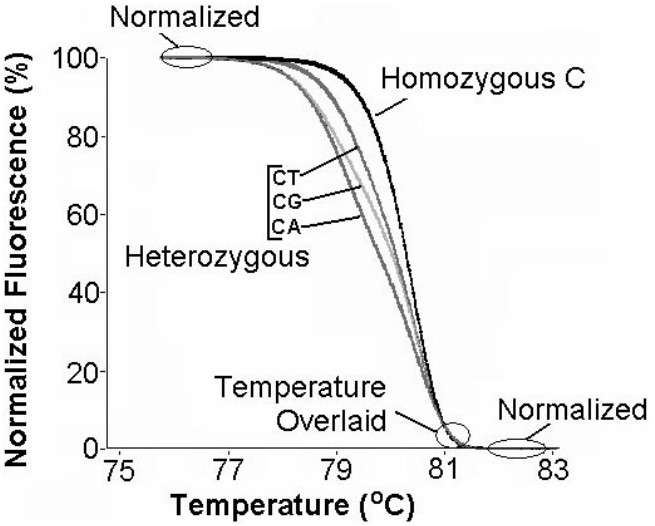

Fig. 2. Representative melting curves of a 100-bp homozygote and its heterozygotes, each genotype analysis performed in duplicate.

Melting curve normalization and temperature overlay were performed as described previously *(16)*. The M13 construct (~40% GC) was used with the SNP position in the middle. The regions used for normalization and overlay of the curves are indicated. The homozygotes and all heterozygotes are easily distinguished from each other.

overlaid in the lower temperature region for comparison. In contrast to the smaller 100-bp product, the different heterozygotes do not clearly separate from each other. However, all heterozygotes are clearly differentiated from the homozygous wild type as required for SNP scanning.

To establish SNP scanning sensitivity and specificity, we studied all possible heterozygotes in three different sequence backgrounds, using constructs designed for this

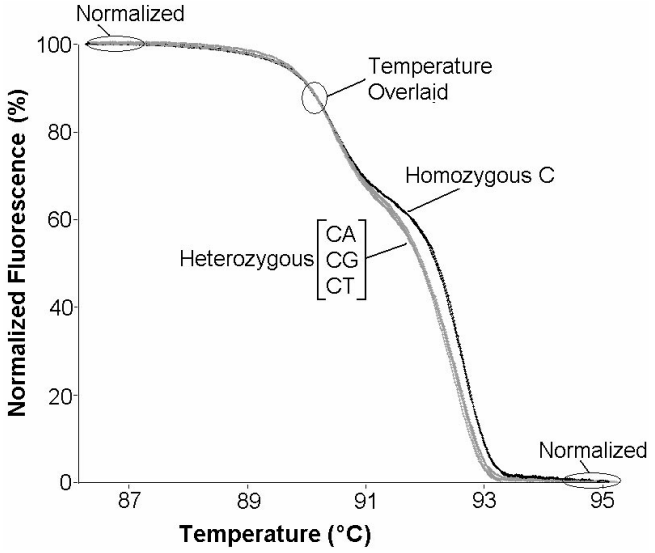

Fig. 3. Representative melting curves of a 600-bp homozygote and its heterozygotes, each genotype analysis performed in duplicate.

The pBR322 construct (~60% GC) was used with the SNP position in the middle. The regions used for normalization and overlay of the curves are indicated. The homozygotes are easily distinguished from the heterozygotes, but the heterozygotes are not distinguishable from each other.

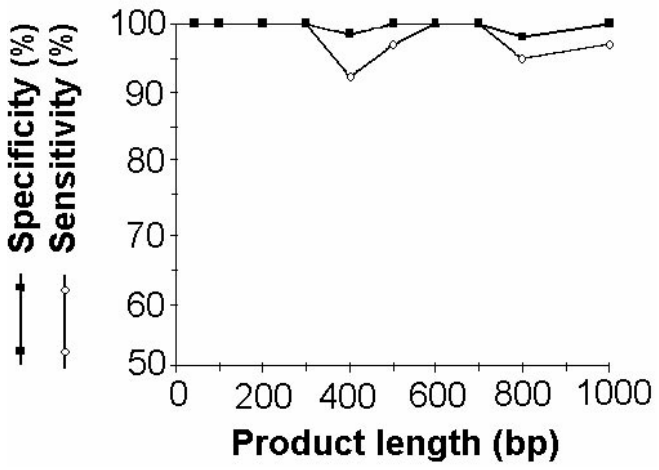

Fig. 4. Effect of product length on the sensitivity and specificity of SNP heterozygote scanning by high-resolution melting.

With the variable site kept near the center, PCR products of ~50, 100, 200, 300, 400, 500, 600, and 800 bp were studied for the M13 (~40% GC), λ (~50% GC), and pBR322 (~60%) sequences. In addition, 700- and 1000-bp PCR products were studied for the M13 sequence, making a total of 26 primer pairs. Twenty-two amplifications were performed with each primer pair, and the samples were grouped to simulate scanning experiments in which 48 decisions of wild type or heterozygous were made by a blinded investigator. The experimental design is detailed in the online Data Supplement.

purpose *(7)*. When we used products 50–1000 bp in length with the SNP centered, there were 14 false negatives (sensitivity, 97.8%) and 2 false positives (specificity, 99.7%) in a total of 1248 cases. The correlation of product length to sensitivity and specificity is shown in Fig. 4. For the 576 cases in which the PCR products were 300 bp or less, all decisions were made correctly. Errors were most frequent for products of 400, 800, and 1000 bp, whereas no errors occurred with products of 600 and 700 bp.

All false negative errors (missed SNPs) of the 1248 centered cases are listed according to background sequence, product size, and SNP type in Table 1. The 14 errors reduced to 7 positions on this matrix because each heterozygote occurs twice (on average) based on the study design. SNPs were missed more frequently in backgrounds of higher AT content and only when the wild type was AA or TT, not CC or GG. The only two false-positive errors (wild-type samples that were called heterozygotes) also occurred with either an AA wild type (M13; 400 bp) or a TT wild type (λ; 800 bp).

Table 1. Background sequence, product length, and SNP type of all false-negative errors of 1248 cases of high-resolution melting analysis for SNP scanning with the variation centered.[a]

Sequence	Length, bp	Wild type	Heterozygote	Errors, n	Cases, n
M13 (40% GC)	400	AA	AG	2	2
	400	AA	AT	1	1
	500	TT	TA	2	3
	1000	AA	AT	2	3
λ (50% GC)	400	TT	TC	3	3
	800	AA	AC	3	3
	800	AA	AG	1	2

[a] Homozygous wild-type samples (AA, CC, GG, or TT) were compared with unknown samples that were either wild type or heterozygous. A false-negative error occurred if a heterozygous SNP was not detected when compared with the homozygous wild-type controls. Each wild type/heterozygote pair was tested one to three times as shown under "Cases" (see online Data Supplement for further details on the study design).

The effect of SNP position on error rate is shown in Fig. 5. The PCR product with the most errors (400-bp M13) was chosen and compared with other products on the same target of the same size that included the variable site. For each product, 22 amplifications and 48 decisions were generated as before. Eight new off-center PCR products produced 384 additional cases. Blinded analysis revealed a sensitivity of 95.6% for these off-center products, greater than the 88% sensitivity obtained with the centered product. These results suggest that there is no clear relationship between the position of the SNP site within the PCR product and scanning sensitivity. Most (six of nine) of the false-negative errors occurred with AA or TT as the known wild type, although three occurred against CC (data not shown). The wild-type (AA) and heterozygote (AC, AG, and AT) melting curves from five PCR products with variable SNP positions (A, B, C, D, and E in Fig. 5) are shown in Fig. 6.

Discussion

To establish the sensitivity and specificity of closed-tube SNP scanning, we used a DNA Toolbox specifically designed to assess scanning techniques *(7)*. Within three sequence contexts of 40%, 50%, and 60% GC content, all four homozygotes and six heterozygotes were constructed by the Toolbox, and scanning experiments were simulated. The effects of PCR product size and position of the base change were studied by placing primers at different positions relative to the sequence variation.

Initially we planned on studying only six primer sets (100–600 bp) for each construct with the variable position near the middle, following the original Toolbox design. However, errors were so infrequent that we extended the study to include 800-bp products for the λ (50% GC) and pBR322 (60% GC) constructs, and 700-, 800-, and 1000-bp products for the M13 (40% GC) construct. In addition, we added primers near to the variable site on each target to study the effects of SNP position, including those very close to the primers.

The DNA Toolbox has been used previously to assess the SNP scanning sensitivity of heteroduplex analysis *(7)* and SSCP analysis *(17)*. The sensitivity of heteroduplex analysis was 92% with no apparent effect of PCR product length or SNP position. The only SNPs missed were those with A:A and T:T mismatches in the heteroduplexes. The sensitivity of SSCP analysis was variable and depended on the separation temperature. Under the best conditions, the sensitivity of SSCP analysis was 94%, although heteroduplex analysis was considered more reliable and robust. The sensitivity of SSCP analysis did not depend on

Fig. 5. Effect of SNP position on the sensitivity and specificity of heterozygote scanning by high-resolution melting.

Starting with the PCR product having the highest error rate [M13 (400 bp); Fig. 4 and Fig. 6C], the positions of the primers relative to the SNP were varied, keeping the length of the product approximately constant. Eight primer pairs were used in addition to the centered pair, testing nine positions approximately equally spaced. Twenty-two amplifications were performed with each primer pair, and the samples were grouped to simulate scanning experiments in which 48 decisions of wild type or heterozygous were made by a blinded investigator. The experimental design is detailed in the online Data Supplement. Representative melting curves for five of the PCR products (*A*, *B*, *C*, *D*, and *E*) are shown in Fig. 6.

the PCR product length, SNP position, or mismatch type. However, better sensitivity was observed with higher GC content. For both heteroduplex and SSCP analysis, sensitivity was established on PCR products of 100–600 bp with the SNP site centered.

In comparison, the sensitivity of high-resolution melting analysis was 98% for a data set that included PCR products up to 1000 bp with the SNP centered. All of the errors were made with PCR products 400 bp or larger, suggesting a dependence on product length. As the product length increases, the difference between wild-type and heterozygote curves became smaller, and the calls seemed to become harder to make. However, the error rate did not consistently increase with lengths above 400 bp. Indeed, the highest error rate occurred at 400 bp (Fig. 4). Errors decreased at 500 bp and were absent at 600 and 700 bp, followed by an increase at 800 and 1000 bp. An interesting observation is that up to 400 bp, the melting curves usually had a single melting transition or domain. At 500–700 bp, most PCR products showed biphasic behavior, similar to the 600-bp product in Fig. 2. Biphasic melting curves are easier to analyze because one domain is usually not affected by the sequence variation, and overlay of the constant domains allows precise comparison of the curve shape in the variable domain. For products 800 bp and above, multiple domains may blur together, producing a complex melting curve. Errors occurred in PCR products with sharp single domains

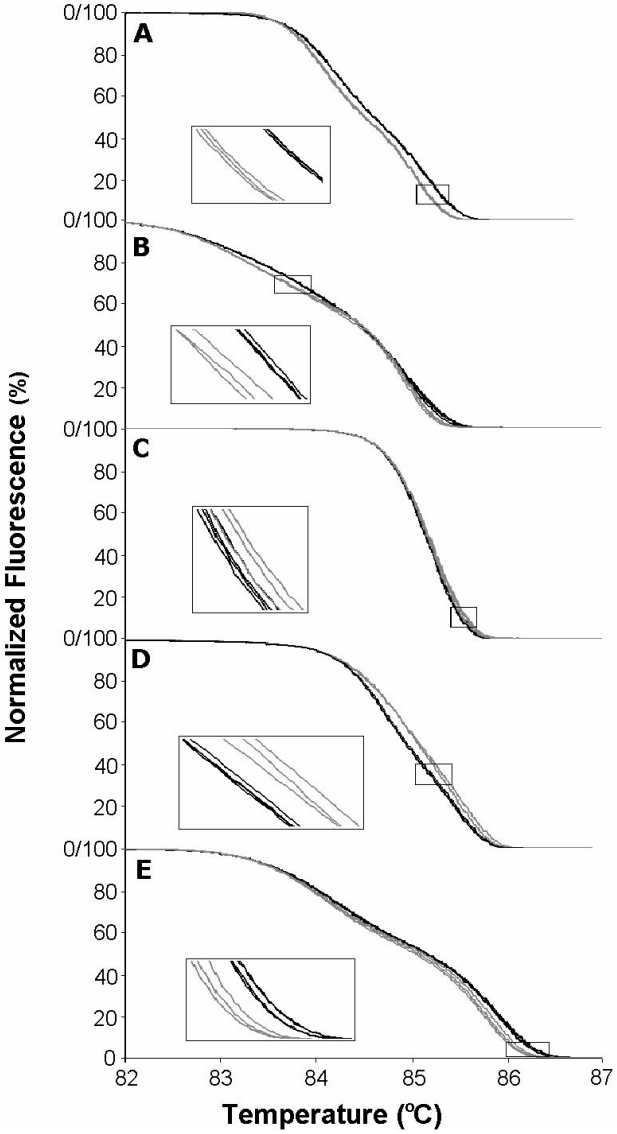

Fig. 6. Normalized, overlaid melting curves for five of the PCR products in the SNP position study (*A*, *B*, *C*, *D*, and *E* in Fig. 5).

The position of the SNP is varied from one end (*A*), through the center (*C*) to the other end (*E*) of the PCR product (see Fig. 5). For all products, the curves were overlaid [temperature shifted; see Ref. *(16)*] between 94% and 97% fluorescence. For each PCR product, four wild-type AA samples are shown in *black*. AC, AG, and AT heterozygotes are shown in *gray* (one sample each). The *insets* are magnifications of one region of each melting curve. One of the heterozygotes in C is not distinguishable from the wild-type samples.

[M13 (400 bp; Fig. 6C); λ (400 bp)] and long products with complex melting curves [M13 (1000 bp); lambda (800 bp)].

Similar to SSCP and heteroduplex analysis, the SNP sensitivity of high-resolution melting did not appear to depend on the SNP position within the PCR product. SNPs near the primers usually altered the low temperature region of the curve, making overlay across this region most effective in showing shape differences (Fig. 6, A and E). Not surprisingly, high-resolution melting resembled heteroduplex analysis more than SSCP analysis in that sensitivity depended on the mismatch type but not the GC content.

SSCP and heteroduplex analysis and high-resolution melting are the only scanning techniques that have been systematically evaluated with the DNA Toolbox. The sensitivities of other common scanning techniques, such as denaturing gradient gel electrophoresis, denaturing HPLC, and temperature gradient capillary electrophoresis, have been estimated on specific genes and can exceed 90% when optimally performed. Proponents of particular methods and commercial interests make objective comparisons difficult.

Sequencing is generally regarded as the gold standard for assessing sequence variation, with accuracy approaching 99.9% for homozygous substitutions *(18)*. However, the sequencing accuracy of SNP heterozygote detection is lower. Furthermore, sequencing accuracy is per base, in contrast to scanning sensitivity, which is per PCR product. For example, a 98% SNP scanning sensitivity for a 200-base fragment (exclusive of primers) is equivalent to a 99.99% sequencing accuracy. Although bidirectional sequencing may achieve this accuracy, the simplicity of scanning methods for ruling out heterozygotes is attractive.

In general, homozygous changes are better determined by sequencing rather than scanning methods. However, any scanning method can detect homozygous sequence variants if the variant is mixed with wild-type DNA. High-resolution melting is unusual among the scanning techniques in that most homozygous changes can be detected without mixing *(11)*. Homozygous changes detected by high-resolution melting have been reported in products >500 bp *(10)*. The sensitivity of detecting homozygous SNP changes could also be studied with use of the DNA Toolbox but was not an objective of the present study.

The use of engineered plasmids for determining scanning error rates has advantages and disadvantages. The ability to systematically study all base changes within several sequence contexts is a distinct advantage. Use of simple plasmids focuses the study on inherent limitations of the scanning techniques rather than on PCR optimization, which is more of a concern with complex genomic DNA. In all cases, scanning techniques are only as good as the PCR amplifications. As a result, the scanning sensitivity on some DNA targets may be less than reported here. Longer products are more difficult to amplify, particularly from complex genomic templates. Until automated analysis methods are developed, the sensitivity of scanning by high-resolution melting will also depend on the experience of the investigator.

Of all available scanning techniques, high-resolution melting is the only method that can be performed in the same container that was used for PCR amplification. Such a closed-tube method requires no processing or automation and is immediately available after scanning for genotyping or sequencing if necessary. When PCR products are not exposed to the environment, contamination concerns are eliminated. Furthermore, high-resolution melting can be performed in ~2 min and appears to have sensitivity comparable or superior to other available scanning techniques.

SNP scanning by melting requires high-resolution analysis to detect the minor melting curve effects of heteroduplexes *(10)*. Real-time PCR instruments are not required and generally lack the necessary resolution for high-sensitivity scanning. Similar to SSCP analysis, mutation scanning by melting requires that unknowns are compared with known wild-type samples. Conveniently, wild-type samples are in abundant supply in most scanning applications.

This research was supported by grants from the State of Utah Centers of Excellence Program, Idaho Technology, the University of Utah Research Foundation, and the NIH (Grant GM072419). Aspects of homogeneous DNA analysis are licensed to Idaho Technology and in turn sublicensed to Roche Applied Science. G.H.R. and C.T.W. have equity interest in Idaho Technology.

References

1. Lay MJ, Wittwer CT. Real-time fluorescence genotyping of factor V Leiden during rapid cycle PCR. Clin Chem 1997;43:2262–7.
2. Crockett AO, Wittwer CT. Fluorescein-labeled oligonucleotides for real-time PCR: using the inherent quenching of deoxyguanosine nucleotides. Anal Biochem 2001;290:89–97.
3. Zhou L, Myers AN, Vandersteen JG, Wang L, Wittwer CT. Closed-tube genotyping with unlabeled oligonucleotide probes and a saturating DNA dye. Clin Chem 2004;50:1328–35.
4. Wittwer CT, Kusukawa N. Nucleic acid techniques. In: Burtis C, Ashwood ER, Bruns DE, eds. Tietz textbook of clinical chemistry and molecular diagnostics, 4th ed. Philadelphia: Elsevier Science, in press.
5. Orita M, Iwahana H, Kanazawa H, Hayashi K, Sekiya T. Detection of polymorphisms of human DNA by gel electrophoresis as single-strand conformation polymorphisms. Proc Natl Acad Sci U S A 1989;86:2766–70.
6. Lerman LS, Silverstein K. Computational simulation of DNA melting and its application to denaturing gradient gel electrophoresis. Methods Enzymol 1987;155:482–501.
7. Highsmith W Jr, Jin Q, Nataraj A, O'Connor J, Burland V, Baubonis W, Curtis F, et al. Use of a DNA toolbox for the characterization of mutation scanning methods. I: construction of the toolbox and evaluation of heteroduplex analysis. Electrophoresis 1999;20:1186–94.
8. Xiao W, Oefner PJ. Denaturing high-performance liquid chromatography: a review. Hum Mutat 2001;17:439–74.
9. Li Q, Liu Z, Monroe H, Culiat CT. Integrated platform for detection of DNA sequence variants using capillary array electrophoresis. Electrophoresis 2002;23:1499–511.
10. Wittwer CT, Reed GH, Gundry CN, Vandersteen JG, Pryor RJ. High-resolution genotyping by amplicon melting analysis using LCGreen. Clin Chem 2003;49:853–60.
11. Liew M, Pryor R, Palais R, Meadows C, Erali M, Lyon E, et al. Genotyping of single-nucleotide polymorphisms by high-resolution melting of small amplicons. Clin Chem 2004;50:1156–64.
12. Zhou L Vandersteen J, Wang L, Fuller T, Taylor M, Palais B, et al. High-resolution DNA melting curve analysis to establish HLA genotypic identity. Tissue Antigens 2004;64:156–64.
13. McKinney JT, Longo N, Hahn SH, Matern D, Rinaldo P, Strauss

AW, et al. Rapid, comprehensive screening of the human medium chain acyl-CoA dehydrogenase gene. Mol Genet Metab 2004;82: 112–20.

14. Willmore BS, Holden JA, Zhou L, Tripp S, Wittwer CT, Layfield LJ. Detection of c-kit activating mutations in gastrointestinal stromal tumors by high-resolution amplicon melting analysis. Am J Clin Pathol 2004;122:206–16.

15. Wittwer CT, Kusukawa N. Real-time PCR. In: Persing DH, Tenover FC, Versalovic J, Tang YW, Unger ER, Relman DA, White TJ, eds. Molecular microbiology: diagnostic principles and practice. Washington, DC: ASM Press, 2004:71–84.

16. Gundry CN, Vandersteen JG, Reed GH, Pryor RJ, Chen J, Wittwer CT. Amplicon melting analysis with labeled primers: a closed-tube method for differentiating homozygotes and heterozygotes. Clin Chem 2003;49:396–406.

17. Highsmith WE Jr, Nataraj AJ, Jin Q, O'Connor JM, El-Nabi SH, Kusukawa N, Garner MM. Use of DNA toolbox for the characterization of mutation scanning methods. II: evaluation of single-strand conformation polymorphism analysis. Electrophoresis 1999;20:1195–203.

18. Ewing B, Hillier L, Wendl MC, Green P. Base-calling of automated sequencer traces using phred. I. Accuracy assessment. Genome Res 1998;8:175–85.